A spectroscopic method for observing the domain movement of the Rieske iron–sulfur protein

Myriam Brugna*†, Simon Rodgers†‡, Anna Schricker*, Guillermo Montoya‡, Michael Kazmeier§, Wolfgang Nitschke*¶, and Irmgard Sinning‡

*Laboratoire de Bioénergétique et Ingénierie des Protéines, Centre National de la Recherche Scientifique, Institut de Biologie Structurale et Microbiologie, 31 chemin Joseph-Aiguier, 13402 Marseille Cedex 20, France; ‡Structural Biology Programme, European Molecular Biology Laboratory, Heidelberg, Meyerhofstrasse 1, 69012 Heidelberg, Germany; and §Laboratoire de Radiobiologie Végétale, Direction des Sciences de la Vie, Département d'Ecophysiologie Végétale et de Microbiologie, CEA, Cadarache, 13108 Saint-Paul-lez-Durance, France

Communicated by Pierre A. Joliot, Institute of Physico-Chemical Biology, Paris, France, December 13, 1999 (received for review July 24, 1998)

The *g*-tensor orientation of the chemically reduced Rieske cluster in cytochrome bc_1 complex from *Rhodovulum sulfidophilum* with respect to the membrane was determined in the presence and absence of inhibitors and in the presence of oxidized and reduced quinone in the quinol-oxidizing-site (Q_o-site) by EPR on two-dimensionally ordered samples. Almost identical orientations were observed when oxidized or reduced quinone, stigmatellin, or 5-(*n*-undecyl)-6-hydroxy-4,7-dioxobenzothiazole was present. Occupancy of the Q_o-site by myxothiazole induced appearance of a minority population with a substantially differing conformation and presence of *E*-β-methoxyacrylate-stilbene significantly reduced the contribution of the major conformation observed in the other cases. Furthermore, when the oxidized iron–sulfur cluster was reduced at cryogenic temperatures by the products of radiolysis, the orientation of its magnetic axes was found to differ significantly from that of the chemically reduced center. The ''irradiation-induced'' conformation converts to that of the chemically reduced center after thawing of the sample. These results confirm the effects of Q_o-site inhibitors on the equilibrium conformation of the Rieske iron–sulfur protein and provide evidence for a reversible redox-influenced interconversion between conformational states. Moreover, the data obtained with the iron—sulfur protein demonstrate that the conformation of ''EPR-inaccessible'' reduction states of redox centers can be studied by inducing changes of redox state at cryogenic temperatures. This technique appears applicable to a wide range of comparable electron transfer systems performing redox-induced conformational changes.

The cytochrome *bc*-complex is the only energy-coupling membrane-integral enzyme common to both photosynthetic and respiratory electron transport chains. In addition to three heme groups, the enzyme contains an unusual [2Fe2S] cluster, the so-called Rieske center. A key enzymatic feature of the complex is the bifurcation of the two electrons derived from oxidation of a quinol molecule at a catalytic site (the ''Q_o-site'') into two distinct electron transfer chains within the complex. The Q_o-site is positioned between a *b*-type heme and the [2Fe2S]-cluster of the Rieske iron–sulfur protein (ISP), and the ISP protein has been shown to play a decisive role in turnover at the site (1). Apart from the physiological quinone, the Q_o-site binds several competitive and noncompetitive inhibitors of catalysis (mostly quinone analogs) such as stigmatellin, 5-(*n*-undecyl)-6-hydroxy-4,7-dioxobenzothiazole (UHDBT), myxothiazole, or *E*-β-methoxyacrylate (MOA) stilbene.

In the recent x-ray structure analyses of the mitochondrial cytochrome bc_1 complex (2–5), the Rieske protein was found in three distinct positions with respect to the remaining subunits of the enzyme, i.e., in a geometry positioning the [2Fe2S]-cluster close to the cytochrome b_L-heme [denoted the ''proximal position'' by Zhang *et al.* (3)], in a second geometry where the cluster is situated in the vicinity of cytochrome c_1 (the ''distal position''), and in a position intermediate between the two extremes [denoted the ''int'' position by Iwata *et al.* (4)]. These three positions were interpreted as representing differing conformational states of the enzyme during turnover, and a domain movement of the Rieske protein was implied as a prerequisite for efficient electron transfer (3–5). A detailed reaction mechanism of Q_o-site turnover based on the three conformational states was proposed by Iwata *et al.* (4), and a crucial role of the protonation state of the histidine ligands to the cluster in this reaction has recently been proposed by Ugulava and Crofts (6, 7). EPR on two-dimensionally ordered samples (8, 9) has been used since the late 1970s to determine the orientations of *g*-tensor directions of the Rieske cluster with respect to the membrane (10–17). Because the different conformations found in the crystals are characterized by significantly altered orientations of the Rieske cluster molecular axes, the proposed variability of conformational states can be observed by EPR on ordered samples, as recently demonstrated on related systems (15–17). In comparison to three-dimensional structure determination, the spectroscopic approach represents a less time-consuming method, allowing the screening of a large number of enzymes and of different states of an enzyme in a short amount of time. We have therefore performed an oriented EPR study on various states of the cytochrome bc_1-complex. The enzyme purified from *Rhodovulum sulfidophilum* (18) was chosen for the experiments described below because of its high stability and an almost fully occupied Q_o-site.

The presence of a number of discrepancies between our results and those of the crystallographic studies furthermore led us to develop a method allowing us to observe otherwise ''EPR-silent'' redox states. This method is likely to be applicable to a wide range of related problems.

Experimental Procedures

Culture Growth and Purification. The bc_1-complex from *Rv. sulfidophilum* was purified according to Montoya *et al.* (18).

Oriented Membrane Multilayers. Oriented samples were obtained as described by Rutherford and Sétif (9). Purified bc_1-complex from *Rv. sulfidophilum* was washed once in 25 mM morpholinepropanesulfonic acid (Mops), pH7, and once in unbuffered water. In the absence of further reductant treatment, the Rieske center was seen to be largely (≈90%) oxidized. For the reduced oriented samples, the bc_1-complex was washed in 25 mM Mops, pH 7/5 mM ascorbate (yielding samples containing reduced Rieske centers but oxidized Q_o-quinone as judged from the

Abbreviations: Q_o-site, quinol-oxidizing site; *Rv.*, *Rhodovulum*; UHDBT, 5-(*n*-undecyl)-6-hydroxy-4,7-dioxobenzothiazole; ISP, Rieske iron—sulfur protein; MOA, *E*-β-methoxyacrylate.

†M.B. and S.R. contributed equally to this work.

¶To whom reprint requests should be addressed. E-mail: nitschke@ibsm.cnrs-mrs.fr.

The publication costs of this article were defrayed in part by page charge payment. This article must therefore be hereby marked "*advertisement*" in accordance with 18 U.S.C. §1734 solely to indicate this fact.

Article published online before print: *Proc. Natl. Acad. Sci. USA*, 10.1073/pnas.030539897. Article and publication date are at www.pnas.org/cgi/doi/10.1073/pnas.030539897

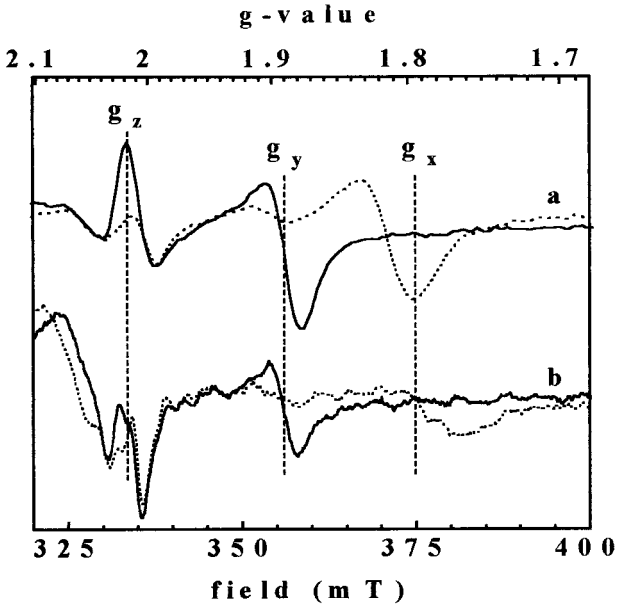

Fig. 1. EPR spectra recorded on oriented multilayers of purified cytochrome bc_1 complex from *Rv. sulfidophilum* with a magnetic field at 0° (continuous lines) and 90° (dashed lines) with respect to the plane of the membrane in the absence of inhibitor (*a*) or in the presence of stigmatellin (*b*). Instrument settings: temperature, 15 K; microwave frequency, 9.43 GHz; microwave power, 6.7 mW; modulation amplitude, 3.2 mT.

position of the g_x-peak at 1.8 in EPR spectra) or in 25 mM Mops/20 mM dithionite (reducing both quinone in the Q_o-pocket and the Rieske centers) and then in unbuffered water. In all these cases, bc_1-complex was subsequently resuspended in unbuffered water in the presence or absence of the inhibitors UHDBT, stigmatellin, myxothiazole, or MOA–stilbene, applied onto sheets of mylar, and dried in a humidity-controlled atmosphere under argon for approximately 72 h at 4°C.

Oriented and nonoriented samples were frozen, kept cooled in a bath of liquid nitrogen, and exposed to γ-irradiation provided by a ^{60}CO-source, at a total dose of 6 kGy. Because the used γ-radiation was found to induce signals in the quartz of the EPR tubes overlapping lines arising from the ISP, the oriented mylar sheets were transferred at 77 K into the EPR tubes after irradiation.

EPR spectra were recorded at liquid-He temperatures by using a Bruker (Karlsruhe, Germany) ESP 300E X-band spectrometer fitted with an Oxford Instruments cryostat and temperature control system.

All chemicals used were reagent grade.

Results and Discussion

***g*-Tensor Orientations of the Chemically Reduced State in the Presence and Absence of Inhibitors.** Fig. 1 shows EPR spectra of oriented samples prepared from (*i*) untreated and (*ii*) stigmatellin-inhibited cytochrome bc_1 complex from *Rv. sulfidophilum* measured with the magnetic field parallel (continuous line) and perpendicular (dotted line) to the plane of the mylar sheets. In the untreated sample, only 10% to 20% of the Rieske centers were in the reduced state (as judged by comparison with ascorbate reduced samples), whereas the complement of Q_o-quinones was fully oxidized as evidenced by the position (g = 1.80) and line width of the g_x-peak (19, 20). As can be seen from the spectra, the samples were well ordered, and the orientations of principal g-tensor axes (Fig. 2) corresponded to those observed previously, i.e., g_x perpendicular and g_z and g_y parallel to the membrane (10–14) both for the untreated and stigmatellin-

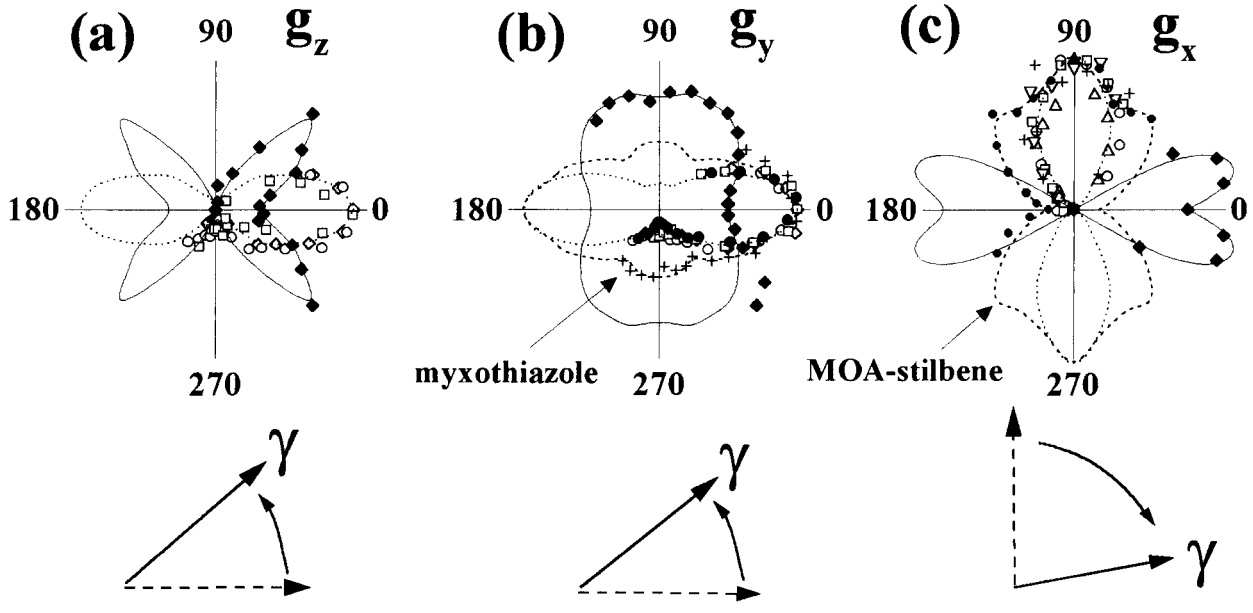

Fig. 2. Orientations of the paramagnetic axes of the Rieske cluster with respect to the membrane plane as measured by the dependences of signal size on the angle between the magnetic field and the membrane. The three signals denoted $g_{x,y,z}$ (see also Fig. 1) correspond to the principal directions of the paramagnetic center (19). Samples oriented in the absence (open diamonds, dotted lines) and in the presence of the inhibitors stigmatellin (open squares, dotted lines), UHDBT (open circles, dotted lines), myxothiazole (crosses, dashed lines) and MOA–stilbene (full circles, dashed lines) were studied. The control sample was furthermore examined with oxidized (open up-triangles, dotted lines) or reduced (open down-triangles, dotted lines) quinone in the Q_o-site (Fig. 2*c*), giving rise to g_x-troughs at differing field positions. Signal amplitudes measured on the irradiation-induced center are denoted by continuous lines and filled diamonds (the g_x-signal was evaluated on the UHDBT-treated sample; see text). (*Lower*) Schematic representation of the directions of these three axes in the chemically (dotted lines) and the irradiation-reduced (continuous lines) states.

inhibited sample. This demonstrates that the orientation of purified complex resulted in two-dimensional ordering similar to that obtained on the parent membranes as already reported by Riedel *et al.* (13) and Rutherford and Sétif (9).

The identical orientations of the uninhibited and the stigmatellin-treated samples are in apparent contradiction to the results observed by x-ray crystallography (3), where the Rieske protein was found in the proximal orientation when stigmatellin was present and in the distal position in the absence of inhibitor. We furthermore determined the *g*-tensor orientation of the UHDBT-, myxothiazole-, and MOA–stilbene-inhibited complexes as well as that of untreated complex under redox conditions where the Q_o-site quinone is fully reduced. In almost all cases (with the exception of myxothiazole and MOA–stilbene; see below), the orientations of *g*-tensors with respect to the mylar sheets were close to identical (Fig. 2, dotted lines). In the presence of myxothiazole, a small broad second maximum of g_y was observed at high angles with respect to the membrane, indicative of the existence of a second population of centers oriented substantially differently from the dominant population. A respective side maximum on g_x could not be detected, probably because of low signal size. g_z was too close to the radical signal to be evaluated with sufficient precision.

In contrast to all these cases, addition of MOA–stilbene resulted in the appearance of a clearly visible side maximum on g_x at about 45° (Fig. 2*c*, dashed line). The apparent amplitudes of the contributions at 90° and 45° are roughly similar, which means that, considering the fact that perpendicular orientations have singularly high signal amplitudes, the 45° orientation represents the dominant population of centers. No obvious additional maximum could be detected in the polar plots of the g_y-signal, suggesting that either the g_y signal is too broad to be detected, or the g_y contribution of the second conformation is contained within the major lobe of the polar plot. In view of the significant signal amplitude of the new conformation in the g_x-region, the latter possibility appears more likely to us. We therefore expect the g_y-orientation to lie at low angles (<30°) with respect to the membrane. Again, a sufficiently accurate evaluation of the g_z-signal was precluded by overlap with the signal of the radicals.

As will be discussed below, myxothiazole and MOA–stilbene were also found by the crystallographic studies to induce conformations different from that obtained in the presence of stigmatellin (3, 5). However, whereas we detect the uninhibited center in the same conformation as in the presence of UHDBT or stigmatellin (in line with Kim *et al.*), other crystallographic studies observed a significant fraction of uninhibited centers in a conformation different from the stigmatellin/UHDBT state. A possible rationalization of this discrepancy consisted of the fact that the crystallographic studies observed the Rieske protein irrespective of the redox state of the cluster, whereas EPR detects only the paramagnetic, i.e., reduced state, of the [2Fe2S] center. To address this question by producing reduced cluster while maintaining the conformation of the oxidized complex, we chose to reduce the cluster by γ-irradiation at cryogenic temperatures.

Low-Temperature γ-Irradiation-Induced Reduction of Samples. Ionizing radiation produces several reactive species, such as hydrogen and hydroxyl radicals or hydrated electrons that are able to change the redox states of metal centers because of their relatively high mobility even at cryogenic temperatures (21, 22). At these temperatures, however, large-scale conformational changes of enzymes are impaired (23, 24), and therefore the protein maintains the conformation of the oxidized state despite reduction induced by the products of radiolysis. We have used oriented and nonoriented samples in a largely oxidized state (i.e., as purified without explicit reduction). In these samples, a small

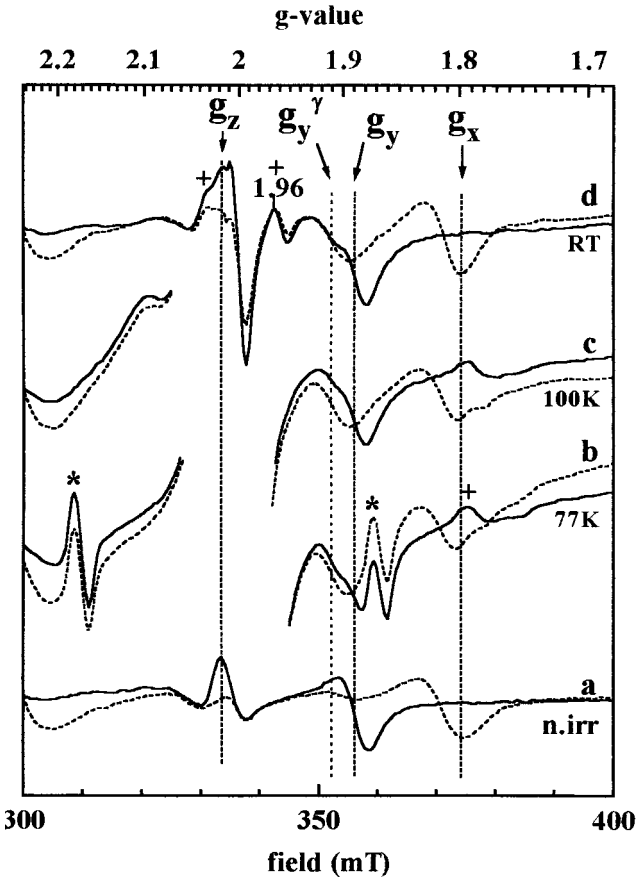

Fig. 3. EPR spectra recorded on nonirradiated (*a*) and γ-irradiated (*b–d*) oriented multilayers of purified cytochrome bc_1 complex from *Rv. sulfidophilum*. Spectra were taken before warming (*b*), after warming to 100 K (*c*) (for 5 min), to 200 K (for 5 min, not shown), and to room temperature (*d*) (for 15 min). Continuous and dashed lines denote spectra taken with the magnetic field parallel and perpendicular to the plane membrane, respectively. Instrument settings are as in Fig. 1.

fraction of the Rieske cluster is in the reduced state (see Figs. 1*a* and 3*a*) providing an internal standard for the orientation. The samples were frozen and cooled to 77 K in a bath of liquid nitrogen. Subsequent exposure to γ-irradiation while maintaining the sample at 77 K resulted in the creation of several new paramagnetic species, most of which were stable only at cryogenic temperatures. The following major paramagnetic species could be identified (Fig. 3): (*i*) A pair of sharp lines (Fig. 3, denoted by *) characterized by a splitting of 50.5 mT and arising from the $H^\cdot$ radical, the splitting into two lines being because of hyperfine interaction between the unpaired electron and the $I = 1/2$ nuclear spin of the hydrogen atom (21). This radical was stable only up to about 100 K. (*ii*) The spectrum of the $OH^\cdot$ radical (not visible on the scale of the depicted spectra) (22), which was seen to be stable up to about 200 K; and (*iii*) three pairs of lines (symmetrical about $g = 2$, 3 lines are outside the depicted spectral region, the visible lines are denoted by "+" in Fig. 3) corresponding to a triplet spin state (the characterization and identification of this species will be described elsewhere). This species was stable up to room temperature and slowly diminished only when the sample was kept at room temperature for several minutes. All these paramagnetic species were found after γ-irradiation of both oxidized and ascorbate-reduced samples (not shown), i.e., did not depend on the redox state of the Rieske cluster. The line at $g = 1.915$ (marked g_y^γ), additional

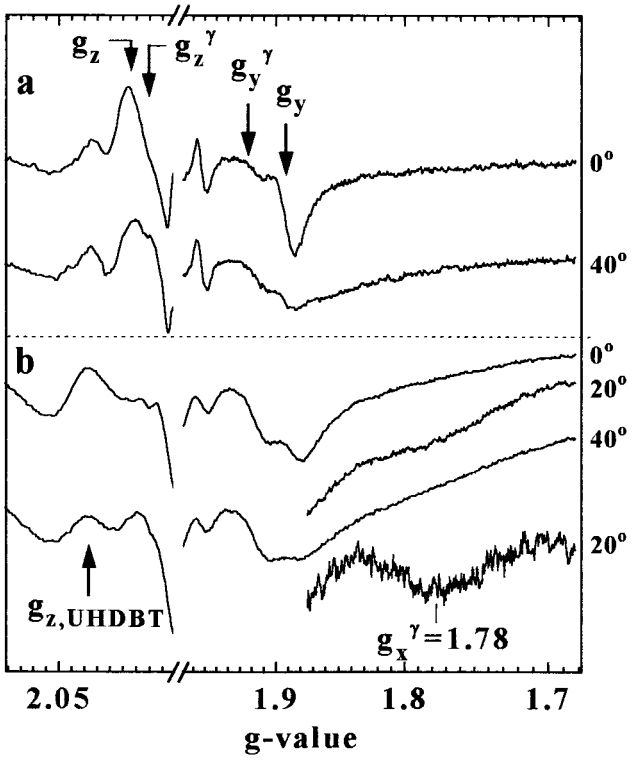

Fig. 4. EPR spectra recorded on oriented samples prepared in the absence of inhibitor (*a*) and presence of UHDBT (*b*) at angles between magnetic field and plane of the membrane as indicated. The bottom trace in *b* represents a difference between spectra recorded after and before γ-irradiation. This latter trace is expanded 4-fold as compared with the other spectra in *b*. Instrument settings were as described in Fig. 1 apart from a modulation amplitude of 1.6 mT. Note the differing field increments before and after the axis break, yielding a better spectral resolution of the field region of the g_z-lines.

signal amplitude in the region of the g_z-peak, and a very broad trough in the region of $g = 1.78$ (see below), persisted after incubation at room temperature (Figs. 3*d* and 4*b*). Fig. 4 provides a better spectral resolution of the signals observed in the field region of the Rieske cluster. The spectra of Fig. 3 were recorded at conditions maximizing signal amplitudes of all paramagnetic species, i.e., by using a very wide scan (500 mT, only 80 mT of which are represented in the figure) and a high modulation amplitude (3.2 mT). In Fig. 4, the spectral region of the Rieske center was recorded at a modulation amplitude of 1.6 mT, and the resolution of the g_z-peaks is enhanced by representing signals with $g > 2$ on a five-times-expanded field scale. As can be seen from Fig. 4, additional signals at $g = 2.04$ and $g = 2.015$ were induced by irradiation in the vicinity of the Rieske cluster's conventional g_z-signal at $g = 2.025$. The signals at apparent *g*-values of 2.04 and 1.96 of Fig. 4 were induced by radiolysis also in samples where the Rieske cluster was chemically prereduced before irradiation (not shown), and furthermore do not arise from a spin ½ paramagnetic species [these signals in fact represent two partner lines of a triplet spectrum (see above)]. The fact that the remaining spectral features with *g*-values of 2.015 and 1.915 strongly resemble the g_z- and g_y-values of the chemically reduced Rieske cluster (2.025 and 1.90), together with the failure to induce the spectrum by γ-irradiation of samples when the Rieske center was chemically prereduced, demonstrated that this paramagnetic species must represent the fraction of Rieske clusters reduced by the products of radiolysis at cryogenic temperatures (for an identification of the g_x^γ-signal, see below).

Irradiation-Induced Reduction of Inhibitor-Treated Samples. Because in the structures reported by Zhang *et al.* (3) different positions of the Rieske protein were found in the presence and absence of the inhibitor stigmatellin, we performed the radiolysis experiment also on a complex oriented in the presence of inhibitors. Samples prepared in the presence of the inhibitor UHDBT yielded qualitatively similar results to the uninhibited complex but showed a better separation between the g_z-peaks of the chemically and the γ-ray-reduced forms (Fig. 4*b*). The presence of UHDBT in fact displaces the g_z-peak of the chemically reduced cluster to $g = 2.04$ (20), thereby reducing the spectral overlap between g_z and g_z^γ (Fig. 4*b*). In addition, the signal corresponding to the paramagnetic *x*-axis of the γ-ray-reduced cluster was clearly visible in a narrow range of orientations (Fig. 4*b*, 20°-spectrum). Overall, the presence of UHDBT induced only marginal deviations on the orientations as compared with the uninhibited sample (see below). Attempts to observe the respective state on the oxidized form of the stigmatellin-inhibited enzyme (because in the presence of stigmatellin the proximal position was found in the crystal study) were unsuccessful because addition of this specific inhibitor to oxidized samples resulted in the spontaneous reduction of the Rieske cluster. This is because of the dramatic rise in redox midpoint potential of the Rieske cluster induced by stigmatellin, as described previously (25, 26).

g-Tensor Orientation of the Photolysis-Reduced Cluster. As is evident from a comparison of the spectra taken at 0°, 40°, and 90° with respect to the membrane (Figs. 3 *a* and *d* and 4 *a* and *b*), the orientation dependences of the radiolysis-induced signals g_z^γ and g_y^γ were significantly different from those of the respective signals in the chemically reduced state. The orientation dependence of the γ-ray-induced spectrum (continuous lines) is compared in the polar plots of Fig. 2 to that of the chemically reduced species (dotted lines). The *z*- and *y*-directions that are parallel to the mylar sheet in the chemically reduced cluster were found at angles of about 40° to 50° in the radiolysis-reduced center. Because the three principal directions of the *g*-tensor are mutually perpendicular, the x-direction must be expected to be almost parallel to the membrane. A very broad line was indeed observed close to 0° in the uninhibited sample; its low signal intensity, however, precluded a precise evaluation of its orientation. In the UHDBT-treated sample, which showed orientations of g_z^γ and g_y^γ rather similar to those of the uninhibited sample, the g_x-trough was relatively well resolved (Fig. 4) and was found to be maximal at 15° with respect to the mylar sheets (Fig. 2*c*). The x-direction therefore differed by about 75° between both forms of the Rieske cluster (Fig. 2 *Lower*). The drastically altered orientation of the magnetic axes of the γ-ray-reduced cluster as compared with the "normal" orientation is schematically visualized in Fig. 6.

Conformational Relaxation at Room Temperature. In nonoriented samples, the same paramagnetic species as described above were found to be induced by γ-irradiation when the spectra were recorded after irradiation without allowing the sample to warm up. By contrast, when the nonoriented sample was thawed, the γ-ray induced spectrum disappeared concomittantly, with an increase of the spectrum corresponding to the chemically reduced form (Fig. 5*a*) demonstrating that the γ-ray induced spectrum actually arose from Rieske centers in an altered conformation. Thawing of the sample allows the radiolysis-reduced Rieske centers to flip to the equilibrium conformation of the chemically reduced iron–sulfur cluster. This relaxation, however, was hampered in the oriented samples, because both

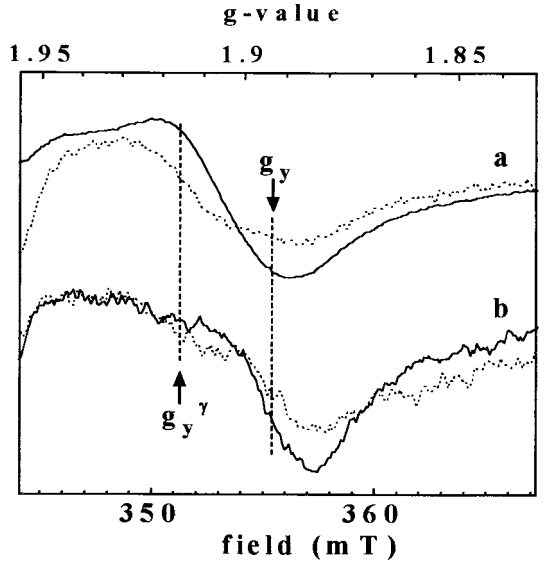

Fig. 5. EPR spectra recorded after γ-irradiation of (*a*) unoriented bc_1 complex before (dotted line) and after (continuous line) incubation at room temperature and of (*b*) oriented sample before (dotted line) and after (continuous line) rehydration. Instrument settings are as in Fig. 1.

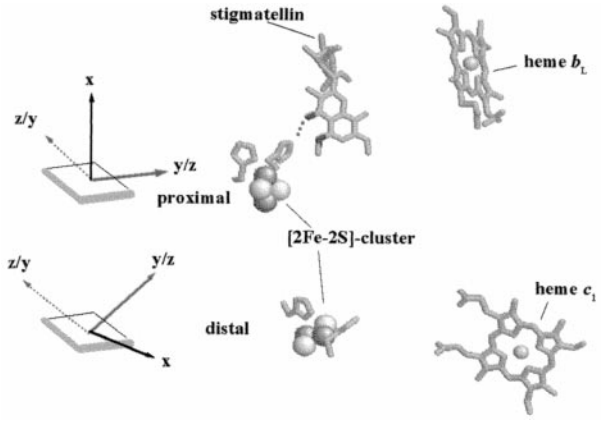

Fig. 6. Schematic representation of the Rieske cluster's magnetic axes with respect to the membrane in the chemically (*Upper*) and the irradiation-reduced (*Lower*) state as compared with the two different (proximal and distal) conformational states observed in the crystal structures (Protein Databank entries 3bcc and 1bcc). Only heme b_L, heme c_1, the inhibitor stigmatellin occupying the Q_o-site, and the two conformational states of the [2Fe-2S]-cluster of the ISP (together with the two ligating histidine residues) are shown.

spectral shape and orientation of the low temperature-reduced Rieske clusters persisted after prolonged incubation at room temperature (Figs. 1 and 3*d*). The inability to relax to the chemically reduced form in oriented samples was found to be at least partially caused by the reduced water content in the dehydrated multilayers. Rehydration of the γ-irradiated oriented samples resulted in a partial conversion of the γ-ray-induced orientation into that of the chemically reduced form (Fig. 5*b*). This conversion was incomplete because (*i*) the water applied to the dried samples affects only the upper layers and does not penetrate down to the bottom of the multilayered sample, and (*ii*) there is a certain probability of radical-induced crosslinking between the Rieske protein and neighboring subunits. Indeed, the nonoriented sample also shows incomplete relaxation to the chemically reduced form (Fig. 5*a*).

Correlation of Observed *g*-Tensor Orientations to Conformational States. Three independent lines of reasoning suggest a specific attribution of the two conformations of the Rieske cluster's magnetic axes observed by EPR to the proximal and distal geometries seen in the crystal structures (3–5). First, in the proximal position of the crystallographic studies, all three symmetry axes of the cluster that are expected to be roughly collinear with the structural symmetry axes (27) are either perpendicular or parallel to the plane of the membrane, whereas the distal position points these axes at oblique angles to the membrane (3). [The geometric symmetry axes of the Rieske cluster correspond to (*i*) the Fe-Fe-direction; (*ii*) the vector going through the two acid-labile sulfur atoms; and (*iii*) the orthogonal direction with respect to *i* and *ii* represented by the vectors joining either the two N(his)- or the two S(cys)-ligands to the cluster.] The same pattern of orientations is found for the chemically and the irradiation-reduced EPR species, respectively (Fig. 6). Second, the chemically reduced EPR species in the presence of oxidized quinone (Fig. 2, open up-triangles) has been shown to interact with the quinone molecule in the Q_o-site (14, 19, 20). This indicates a close vicinity of the Rieske cluster to this site and corresponds to the proximal position seen in the structure. Third, the presence of the inhibitors stigmatellin (3, 5) and UHDBT (5) was reported to induce the proximal conformation, whereas MOA–stilbene was seen to favor the distal conformation. In the EPR experiments, the *g*-tensor orientations observed in the presence of both stigmatellin and UHDBT corresponded to those of the chemically reduced states, whereas in the presence of MOA–stilbene, an oblique orientation was observed.

The paramagnetic *x*-axis of the Rieske cluster would thus be expected to be collinear with the Fe-Fe-axis (cf. Fig. 6), resolving a long-standing controversy concerning the attribution of this axis (27–29). The two remaining axes cannot be assigned from our data, because in both the chemically reduced and the γ-ray reduced Rieske clusters, the angles of the *y*- and *z*-axes are roughly similar with respect to the membrane. The tilt angle of 57° seen in the structural work is intermediate between that observed on going from the chemically to the γ-ray reduced species (75°) and that found between the uninhibited and the MOA–stilbene treated states (45°).

Comparisons Between the EPR Data and the Results of the Crystal Structures. In the structural studies (3–5), the equilibria between the different conformations were interpreted as being influenced by the presence and nature of Q_o-site inhibitors. The EPR results corroborate these conclusions, showing that the presence of myxothiaxole or MOA–stilbene alters the equilibrium between these states as compared with the enzyme with a Q_o-site occupied by quinol, quinone, stigmatellin, or UHDBT.

In the crystal structures from different groups (cf. 3–5), the position of the ISP in the uninhibited enzyme, however, appears rather variable. The EPR results suggest a rationalization for this finding, because in the reduced state of the cluster we detect the ISP in the proximal position, whereas when the cluster is oxidized, it appears to be close to what has been defined as distal positions by the structural articles. According to the EPR results, the position of the ISP in the complex is therefore at least partially controlled by the redox state of the [2Fe-2S]-cluster. The discrepancies in structures between different groups may thus be caused by inequivalent reduction states of the ISP.

This raises the question in which way the redox state of the iron–sulfur cluster can possibly influence the conformational equilibrium.

The model for the initial steps of quinol-oxidation as proposed by Ugulava and Crofts (6) suggests a structural interpretation for these phenomena. In their model, binding of quinol and subsequent reduction of the ISP require that the histidine ligand of the

cluster that interacts with the quinol must be deprotonated to allow formation of a hydrogen bond between the quinol's hydroxy group and the deprotonated nitrogen of the imidazole moiety. Both in the structural studies and in the EPR experiments, pH values are roughly neutral, so that in the oxidized state of the cluster, the histidine ligand will be partly protonated and partly deprotonated (the pK of the histidine is close to 8). With the exception of the EPR data on reduced quinone (see Fig. 2), ambient potentials are such that the quinone will be quantitatively oxidized. The fraction of ISP having a protonated histidine ligand will now be able to engage in a hydrogen bond with an oxygen of oxidized quinone, locking the ISP in the proximal position. The remaining part of ISP will lack this interaction and therefore will be present in one (or more) of the distal positions. In the reduced state of the cluster, however, the pK of the proton on histidine is significantly upshifted, resulting in spontaneous protonation of the histidine ligand on reduction of the cluster. In this state, all ISP will be observed in the proximal position in line with the EPR data. According to this model, one might expect the reduced ISP to go to the distal state in the presence of quinol, a fact that we do not observe. However, in this state, no strong interaction between quinone and the iron–sulfur cluster occurs, as witnessed by the absence of the narrow $g_x = 1.8$ signal. This argues for a more distant position of the quinol with respect to the iron–sulfur cluster in this state. The differing position may be induced by interaction of the opposite hydroxyl group with another hydrogen-bridge acceptor [see the recent work by Crofts *et al.* (7)].

A substantial role of the proton on the N^{ε}-histidine with respect to binding of quinone analogs in the Q_o site and on stabilization of the ISP in the different conformational states has recently been demonstrated also for the cytochrome b_6f complex (16).

Conclusions

Until recently, it has been assumed that proteins involved in electron transport have to be rather rigid to allow efficient electron transfer rates. A long-range domain movement, as shown in this work and postulated already from the crystal structures (3) for the cytochrome bc_1 complex, represents a different mechanism for bridging long distances between redox centers. In the bc_1 complex, the extrinsic domain of the Rieske protein nods like a "pump head" to transfer electrons from the quinone in the Q_o-site to cytochrome c_1. The method of γ-ray-induced reduction described here has been applied to cytochrome *bc*-type complexes from evolutionary distant species (Archaebacteria, higher plants, etc.), all of which show similar behavior (detailed reports will be presented elsewhere). The method using radiolytic reduction at cryogenic temperatures together with EPR spectroscopy represents a quick and generally applicable technique for a wide range of redox proteins. In particular, it allows one to tackle problems that could not be studied so far when the samples were EPR silent.

We thank A. W. Rutherford (CEA, Saclay, France) for familiarizing us with the secrets of partially dehydrated multilayers and for numerous hints and suggestions; E. Berry (Lawrence Berkeley National Laboratory, Berkeley, CA), A. R. Crofts (University of Illinois, Urbana, IL), and T. A. Link (Universitäts Klinikum, Frankfurt, Germany) for stimulating discussions and communicating data before publication; and A. Boussac (Saclay, France) and R. Kappl (Uniklinikum Hamburg, Hamburg, Germany) for advice concerning the radiolytic method. Thanks are furthermore due to B. Guigliarelli and P. Bertrand (CNRS, Marseille, France) for contributing theoretical expertise on iron–sulfur clusters, to A. Verméglio (Cadarache) for suggesting the γ-ray source at Cadarache, and to the EPR group at the Institut de Biologie Structural et Microbiologie (Marseille) for extensive access to the EPR facilities. This work was supported by a Deutsche Forschungsgemeinschaft Fellowship to S.R., a Human Capital and Mobility Program fellowship to G.M. (ERBCHBCIT941622), and by the European Commission (BIO2-CT93–0076).

1. Trumpower, B. L. & Edwards, C. A. (1979) *J. Biol. Chem.* **254,** 8697–8706.
2. Xia, D., Yu, C.-A., Kim, H., Xia, J.-Z., Kachurin, A. M., Zhang, L., Yu, L. & Deisenhofer, J. (1997) *Science* **277,** 60–66.
3. Zhang, Z., Huang, L., Shulmeister, V. M., Chi, Y.-I., Kim, K. K., Hung, L.-W., Crofts, A. R., Berry, E. A. & Kim, S.-H. (1998) *Nature (London)* **392,** 677–684.
4. Iwata, S., Lee, J. M., Okada, K., Lee, J. K., Iwata, M., Rasmussen, B., Link, T. A., Ramaswamy, S. & Jap, B. K. (1998) *Science* **281,** 64–71.
5. Kim, H., Xia, D., Yu, Ch.-A., Xia, J.-Z., Kachurin, A., Zhang, L., Yu, L. & Deisenhofer, J. (1998) *Proc. Natl. Acad. Sci. USA* **95,** 8026–8033.
6. Ugulava, N. B. & Crofts, A. R. (1998) *FEBS Lett.* **440,** 409–413.
7. Crofts, A. R., Hong, S., Ugulava, N., Barquera, B., Gennis, R., Guergova-Kuras, M. & Berry, E. A. (1999) *Proc. Natl. Acad. Sci USA* **96,** 10021–10026.
8. Blasie, J. K., Erecinska, M., Samuels, S. & Leigh, J. S. (1978) *Biochim. Biophys. Acta* **501,** 33–52.
9. Rutherford, A. W. & Sétif, P. (1990) *Biochim. Biophys. Acta* **1019,** 128–132.
10. Prince, R. C., Crowder, M. & Bearden, A. J. (1980) *Biochim. Biophys. Acta* **592,** 323–337.
11. Hootkins, R. & Bearden, A. (1983) *Biochim. Biophys. Acta* **723,** 16–29.
12. Prince, R. C. (1983) *Biochim. Biophys. Acta* **723,** 133–138.
13. Riedel, A., Rutherford, A. W., Hauska, G., Müller, A. & Nitschke, W. (1991) *J. Biol. Chem.* **266,** 17838–17844.
14. Liebl, U., Pezennec, S., Riedel, A., Kellner, E. & Nitschke, W. (1992) *J. Biol. Chem.* **267,** 14068–14072.
15. Brugna, M., Albouy, D. & Nitschke, W. (1998) *J. Bacteriol.* **180**, 3719–3723.
16. Schoepp, B., Brugna, M., Riedel, A., Nitschke, W. & Kramer, D. M. (1999) *FEBS Lett.* **450,** 245–251.
17. Brugna, M., Nitschke, W., Asso, M., Guigliarelli, B., Lemesle-Meunier, D. & Schmidt, C. (1999) *J. Biol. Chem.* **274,** 16766–16772.
18. Montoya, G., te Kaat, K., Rodgers, S., Nitschke, W. & Sinning, I. (1999) *Eur. J. Biochem.* **259,** 709–718.
19. deVries, S., Albracht, S. P. J. & Leeuwerik, F. J. (1979) *Biochim. Biophys. Acta* **546,** 316–333.
20. Matsuura, K., Bowyer, J. R., Ohnishi, T. & Dutton, P. L. (1983) *J. Biol. Chem.* **258,** 1571–1579.
21. Thomas, J. K. (1969) *Adv. Rad. Chem.* **1,** 103.
22. Spinks, J. W. & Woods, R. J. (1964) in *An Introduction to Radiation Chemistry* (Wiley, New York).
23. Kappl, R., Höhn-Berlage, M., Hüttermann, J., Barlett, N. & Symons, M. C. R. (1985) *Biochim. Biophys. Acta* **827,** 327–343.
24. Leibl, W., Nitschke, W. & Hüttermann, J. (1986) *Biochim. Biophys. Acta* **870,** 20–30.
25. von Jagow, G. & Ohnishi, T. (1985) *FEBS Lett.* **185,** 311–315.
26. Nitschke, W., Hauska, G. & Rutherford, A. W. (1989) *Biochim. Biophys. Acta* **974,** 223–226.
27. Bertrand, P., Guigliarelli, B., Gayda, J.-P., Beardwood, P. & Gibson, J. F. (1985) *Biochim. Biophys. Acta* **831,** 261–266.
28. Gurbiel, R. J., Batie, C. J., Sivaraja, M., True, A. E., Fee, J. A., Hoffman, B. M. & Ballou, D. P. (1989) *Biochemistry* **28,** 4861–4871.
29. Link, T. A. & Iwata, S. (1996) *Biochim. Biophys. Acta* **1275,** 54–60.